APPLIED ORGANOMETALLIC CHEMISTRY, VOL. 11, 195–203 (1997)

$Cp_2\overline{TiCH_2Si(Me_2)}NSiMe_3$: A Single-Source Precursor to Titanium-based Ceramic Thin Films by Chemical Vapor Deposition

Benoit Chansou, Robert Choukroun and Lydie Valade*
Equipe 'Précurseurs Moléculaires et Matériaux', CNRS — Laboratoire de Chimie de Coordination, 205 route de Narbonne, 31077 Toulouse Cedex, France

The four-membered-ring heterocyclic molecule $Cp_2\overline{TiCH_2Si(Me_2)}NSiMe_3$ (1; $Cp = \eta - C_5H_5$) was studied as a single-source precursor to titanium-based ceramic thin films. Its decomposition was studied at atmospheric and low pressure under nitrogen, argon and helium by TG–DTA–MS. Thin films containing the four elements of the metallacycle and oxygen were deposited on silicon substrates by low-pressure (20 Torr) chemical vapor deposition (CVD) between 773 and 923 K. Films were characterized by SEM–EDS, XPS, EPMA–WDS and XRD analyses. © 1997 by John Wiley & Sons, Ltd.

Keywords: OMCVD; ceramic; thin films; metallacycle; titanium

* Author to whom correspondence should be addressed.

INTRODUCTION

Organometallic chemical vapor deposition (OMCVD) has gained increasing interest during the last 30 years because the use of molecular percursors for the preparation of ceramic materials offers advantages over conventional high-temperature processes with regard to homogeneity, purity, partical size regulation and amenability to intelligent processing control.[1–6] Moreover, single-source precursors, i.e. molecules exhibiting prebonding between the atoms from which the ceramic will form, have lately been extensively studied as they should require lower energy to convert them into ceramic materials than conventional precursors.[7,8]

The $Cp_2\overline{TiCH_2Si(Me_2)}NSiMe_3$ molecule, **1**($Cp = \eta - C_5H_5$), exhibits a four-membered ring arrangement that prompted us to check whether it could be used as a single-source precursor to advanced ceramic thin films containing the atoms of the ring. Thin films of titanium carbide, nitride and silicide are interesting in many ways for mechanical and/or electrical applications.[9–11]

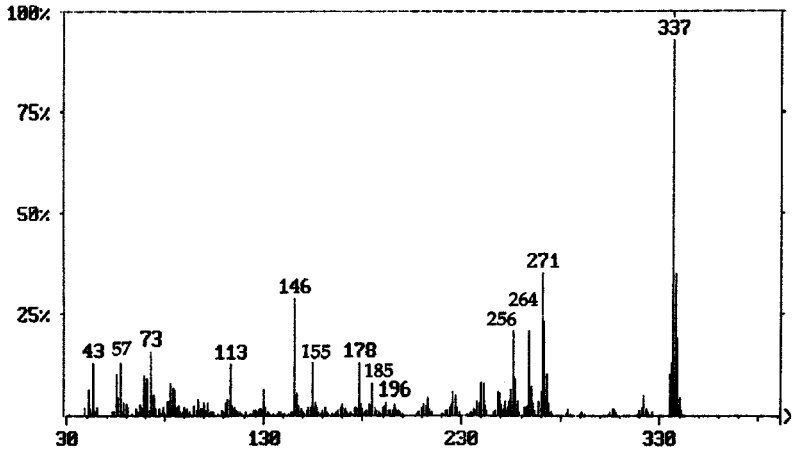

Figure 1 EI mass spectrum of $Cp_2\overline{TiCH_2Si(Me_2)}NSiMe_3$.

CCC 0268–2605/97/030195–09 $17.50

Received 31 October 1995
Accepted 18 April 1996

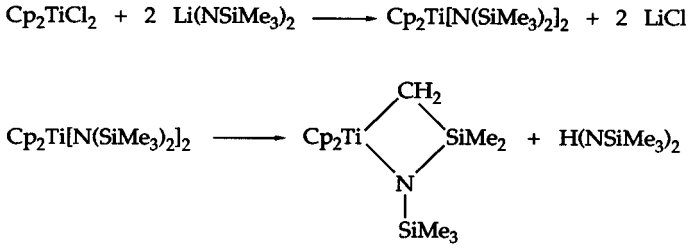

Scheme 1

Combination of these properties can be foreseen if solid solutions or defined phases can form. The Ti–Si–N system is technologically interesting for electrical interconnections in electronic devices,[12] while the Ti–Si–C system attracts interest for its mechanical properties.[13,14] The phase diagrams of these two systems have been studied[15,16] and chemical vapor deposition (CVD) has been used to deposit thin films from conventional precursors.[13,14,17–20] The quaternary Ti–Si–C–N system that may arise from the decomposition of compound **1** could hopefully combine the electronic and unusual mechanical properties afforded by both of the systems mentioned above.

This paper is intended to show that compound **1** can be used as a single-source precursor to ceramic thin films containing titanium, silicon, carbon, nitrogen and oxygen.

RESULTS AND DISCUSSION

Synthesis and characterization of 1

$Cp_2TiCH_2Si(Me_2)NSiMe_3$ (**1**) was prepared following reported procedures (Scheme 1).[21,22] Sublimation (383 K/10^{-3} Torr) affords **1** as a waxy red compound that cannot be crystallized. Elemental and ^{1}H NMR analyses were consistent with previously reported data.

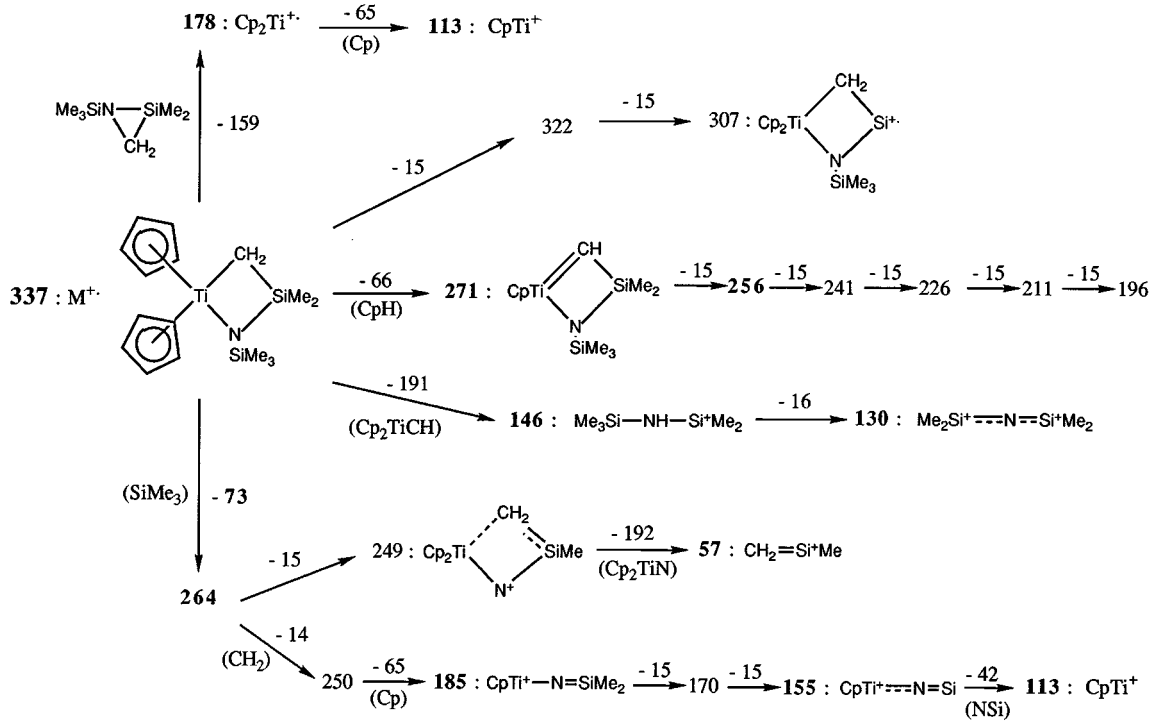

Scheme 2

Mass spectrometry of **1** (Fig. 1) shows the parent peak at $m/z = 337$. Major fragments have been assigned following Scheme 2. It should be noted that a number of these fragments exhibit the Ti–Si–C–N cycle, or at least contain all four elements. The chemical structures proposed in Scheme 2 take into account the comparison of the observed peak pattern with the theoretical isotopic distribution of titanium and other elements. Species containing only silicon and carbon or only silicon and nitrogen were also identified. Note that if these species also arise under thermal fragmentation of **1** they may induce the formation of silicon carbide or nitride.

Thermal decomposition of 1

The thermal behavior of **1** was studied under nitrogen, helium and argon. At atmospheric pressure and under nitrogen as well as under argon (Fig. 2a), a one-step 73% weight loss is observed within the 473–603 K temperature range. The compound does not melt (no DTA peak prior to weight loss). The DTA curve exhibits two thermal events correlated to the weight loss (Fig. 2a): an endothermic peak at 523 K and an exothermic one at 573 K. Under helium, the overall weight loss remains identical but occurs in two steps (Fig. 2b). The two thermal events observed under argon are present

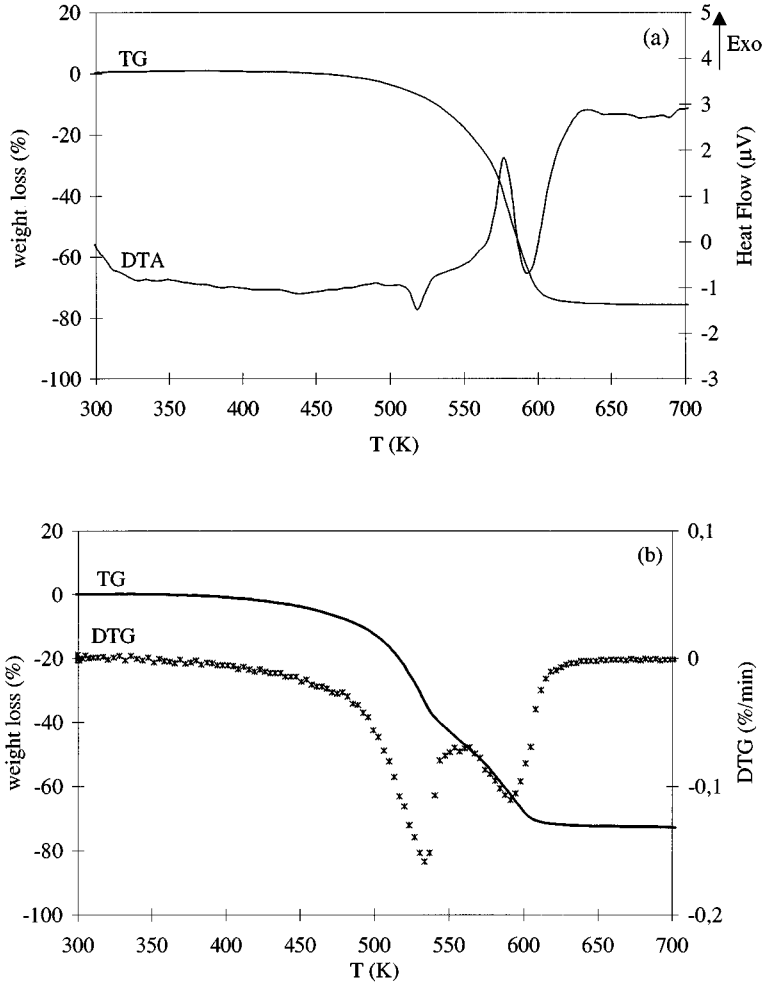

Figure 2 Thermogram of $Cp_2\overline{TiCH_2Si(Me_2)}NSiMe_3$: 10 K min^{-1} temperature ramp. (a) Weight loss and DTA curves for argon and P_{atm}. (b) Weight loss and DTG curves for helium and P_{atm}.

at the same temperatures and might be assigned to each weight loss. In conditions closer to those of the CVD experiments, i.e. at low pressure and under nitrogen, a single weight loss is observed again and reaches 100%.

Coupled MS analysis of the gas phase, performed under N_2, indicates the presence of $[Me_3Si^+]$ ($m/z=73$), $[Cp^+]$ ($m/z=65$) and $[HNSi_2Me_5^+]$ ($m/z=146$) as major decomposition products. $[Me_3Si^+]$ and $[Cp^+]$ fragments appear at the beginning of the weight loss, i.e. at *ca* 473 K, while $[HNSi_2Me_5^+]$ is detected at *ca* 573 K (end of weight loss). The fragments resulting from the thermal decomposition of **1** are also present among the major species detected in the conditions of electron impact (EI) mass spectrometry fragmentation. This further allows us to propose the following pathway for the decomposition of **1**: the Cp and Me_3Si groups are eliminated in the first step of the decomposition while the four-membered ring core of the molecule remains stable up to higher temperatures. This pathway is consistent with the two-step weight loss shown under helium and with the two thermal events described above.

Figure 3 shows the thermal behavior of **1** recorded in isothermal mode under nitrogen. At atmospheric pressure, the weight loss varies linearly as a function of time at 413 and 433 K (Fig. 3a). This behavior corresponds to a zero-order kinetic process, consistent with the simple sublimation of the compound. At 443 K and

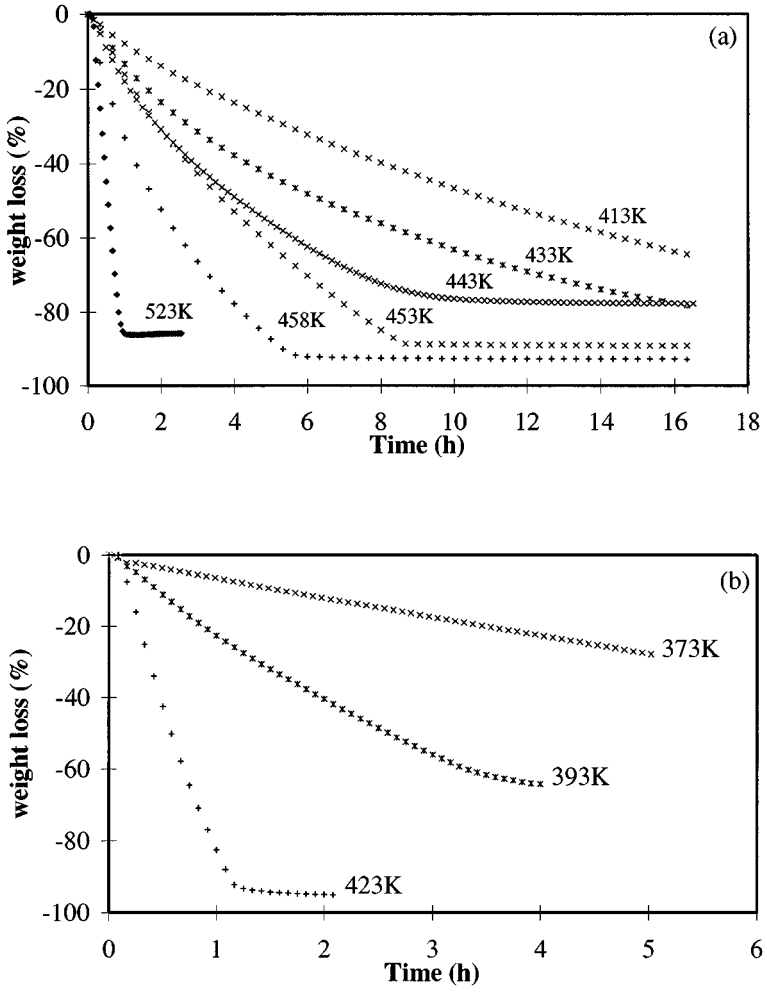

Figure 3 Thermogram of $Cp_2TiCH_2Si(Me_2)NSiMe_3$ showing the weight loss at various temperature levels. N_2 carrier gas ($1\ l\ h^{-1}$). (a) P_{atm}. (b) $P=5$ Torr.

Table 1. CVD from $Cp_2\overline{TiCH_2Si(Me_2)}NSiMe_3$[a]

Sample no.	Mass of precursor (mg)	Substrate type	Substrate temperature T_s(K)	Analysis of the deposits(at %)				
				Ti	Si	C	N	O
1	170	Si	923	14	20	7	1	58
2	130	Si	873	17	17.5	12	1.5	52
3	120	Si	823	20	13	14	2	51
4	170	Si	773	19	10	28	4	39
5	1360	Si, *steel*	773	*13*	*7*	*15*		*65*

[a] N_2 flow rate: 5 l h^{-1}; *P*: 20 Torr. Samples 1 to 4 were analysed by XPS after a 10 min sputtering at 4 kV. Analysis of sample 5 was carried out by EPMA–WDS on the deposit obtained on a 35CD4 steel substrate.

above, the formation of a residue (10–20%) indicates the decomposition of **1**. At low pressure (Fig. 3b), the same phenomena are observed. However, the beginning of decomposition is shifted towards a lower temperature (393 K).

This thermal study indicates that **1** bears the features (volatility and decomposition ability) necessary for use as a CVD precursor. Moreover, we could study, under nitrogen and as a function of the vaporization temperature, the nature of the gas phase. During CVD experiments, **1** can be transported in sublimation mode up to 433 K at atmospheric pressure and up to 383 K at low pressure. Above these temperatures, the gas phase will consist of the decomposition products of the molecule as identified by conventional dynamic thermal analysis (*vide supra*).

Thin-films deposition and characterization

In an attempt to confirm the ability of **1** to form ceramic thin films, and to identify the atoms that would participate in the deposit, hot-wall CVD experiments were carried out on silicon substrates, under nitrogen, and at low pressure. The two driving modes (sublimation and decomposition) were studied but could not be accurately compared because, in hot-wall CVD equipment, the presence of a large zone of temperature gradient leads in any case to the decomposition of the vapor before it reaches the substrate surface. Therefore, we report here only on the studies of the films obtained in decomposition mode (precursor vaporized at 423 K) for various substrate temperatures (773–923 K). The experimental conditions and the analyses of the deposits are gathered in Table 1.

The atomic compositions of the deposits were estimated by XPS analysis (Table 1). The XPS spectrum of sample 4 (Fig. 4) is representative of the deposits obtained for all substrate temperatures. The deconvolution of the C_{1s} and Ti_{2p} peaks is presented in Fig. 5. All deposits contain titanium, silicon, carbon, oxygen and small amounts of nitrogen. The observed binding energies for each element are reported in Table 2 and their values can be compared with those in the literature.[23,24] The position of the titanium peak is consistent with the presence of titanium dioxide and titanium oxycarbide or oxynitride. Silicon is also present as an oxycarbide and does not appear as titanium silicide. Nitrogen is present in small amounts and from its binding energy it may be inferred that it appears in a

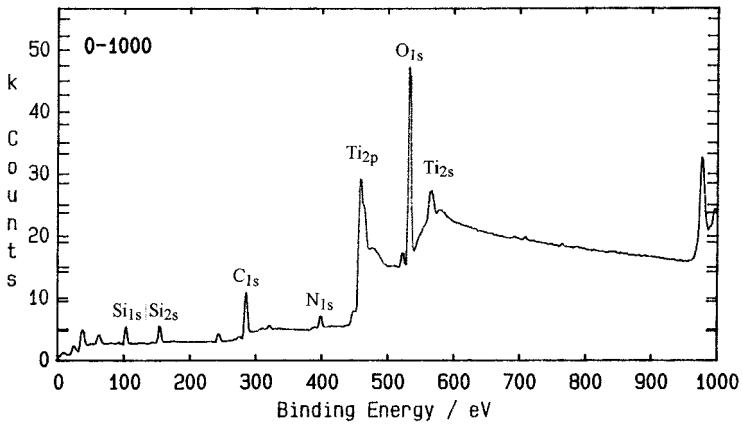

Figure 4 XPS spectrum of Sample 4.

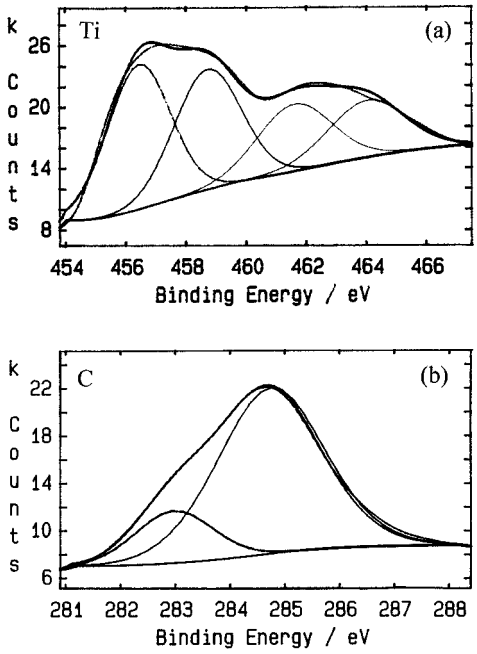

Figure 5 Measured XPS spectra of the Ti_{2p} doublet (a) and C_{1s} peak (b) in sample 4.

nitrogen-rich titanium oxynitride phase. The binding energies observed for carbon are consistent with the presence of amorphous carbon and carbide as titanium and/or titanium oxycarbide. Therefore, the deposits can be described as titanium and silicon oxycarbides and nitrides containing titanium dioxide and amorphous carbon.

The oxygen content of the deposits is high at all substrate temperatures (40–60 at %). Precursor **1** is highly sensitive to oxygen and moisture, and an imperfect purification of the CVD apparatus (which is equipped with only a primary pumping system — see Experimental section) is sufficient to explain the incorporation of oxygen in the deposits. Prolonged sputtering of the surface of the deposits during XPS analysis does not eliminate oxygen. Electron microprobe analysis with wavelength-dispersive spectrometry (EPMA–WDS) of sample 5, prepared in the same conditions as sample 4, on silicon and 35CD4 steel substrates, confirms the presence of oxygen in the bulk of the deposits (Table 1). Scanning electron microscopy (SEM) of sample 5 shows that the deposits are *ca* 0.9 μm thick (Fig. 6) and exhibit a similar homogeneous granular surface on both types of substrates (Fig. 7). As shown on Fig. 8, crystallized phases are formed and the influence of the nature of the substrate is shown by the difference observed in the XRD peaks on each substrate. None of the sets of XRD peaks could be accurately attributed to known phases.

Table 2. XPS binding energies in eV

Phase	Si_{2p}	C_{1s}	N_{1s}	$Ti_{2p_{3/2}}$	O_{1s}
Titanium				453.8	
Amorphous carbon		284.5			
β-SiC	100.5	283.5			
SiC_xO_y	102.0	284.6			532.1
SiO_2	103.4				532.4
SiN_xO_y	102.0		398.3		532.2
α-Si_3N_4	101.4		397.9		
TiC		281.2		454.7	
TiN			396.7	454.6	
TiN_xO_y			398.6	455.4	
TiO_2				458.5	530.0
$TiSi_2$	98.3			453.2	
Sample 4	102.4	282.9	397.1	456.4	531.3
		284.7		458.7	

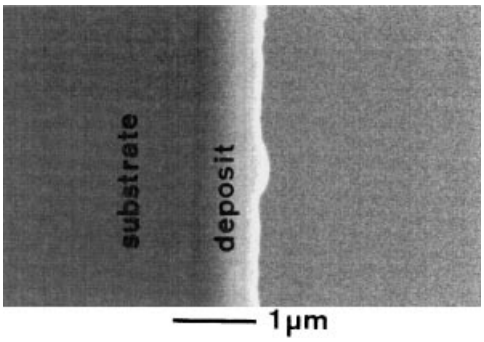

Figure 6 SEM of the cross-section of sample 5. Deposit on silicon substrate.

The preliminary CVD studies conducted on compound **1** have shown its ability to be used as a single-source precursor to the formation of deposits in the Ti–Si–C–N–O system. Further studies, using higher-quality CVD equipment, will be performed to allow the exclusive formation and accurate characterization of Ti–Si–C–N-containing deposits.

EXPERIMENTAL

General comments

All manipulations were carried out by using standard Schlenk and dry-box techniques under

argon. Pentane was dried and distilled over Na/K alloy. Compound **1** was prepared following reported procedures.[19,20] Attempts to crystallize it by various techniques (sublimation, recrystallization) did not success in producing crystals suitable for X-ray diffraction studies. The ^{1}H NMR spectrum was recorded on a Bruker AMX200 (200 MHz) spectrometer. Mass spectrometry (MS) analyses were conducted on a Nermag Model R10-10 spectrometer.

SEM observations of the deposits were performed on a JEOL JMS 840A unit equipped with an energy-dispersive spectrometry (EDS) analyser. Their elemental analysis was determined by X-ray photoelectron spectroscopy (XPS) using a VG Escalab Model MK2 (Mg Kα radiation, 1253.3 eV) under sputtering of the surface with an Ar^{+} ion beam. Electron microprobe analyses (EPMA) were performed on a Cameca SX-50 apparatus equipped with three wavelength-dispersive spectrometers (WDS). X-ray data were collected on a Seifert model XRD-3000 diffractometer (Cu radiation) working at the grazing angle (1°) and equipped with a liquid-nitrogen-cooled germanium detector.

Thermoanalytical studies

Thermogravimetric studies were carried out in a Setaram TG-DTA 92 system coupled to a Leybold–Heraeus QX 2000 quadrupolar mass spectrometer through a capillary that allows the gases to enter the analysis chamber continuously. This on-line TG–MS configuration allows us to approach the thermal decomposition of a precursor through simultaneous analysis of the volatile decomposition products. The thermogravimetric equipment offers simultaneous TG and DTA data collection at normal or low pressure with various carrier gases, and from room temperature to 1873 K. Thermal studies were performed in dynamic mode (at a heating rate of 10 K min^{-1}) and in isothermal mode, the latter allowing us to define the temperature domains in which the compound is transported in to the gas phase either by sublimation or decomposition. In

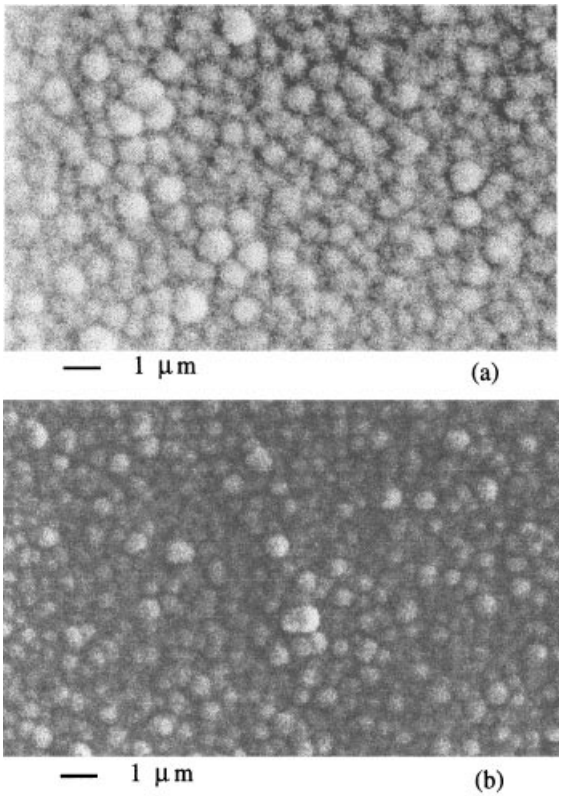

Figure 7 SEM of the surface of sample 5. (a) Silicon substrate. (b) 35CD4 steel substrate.

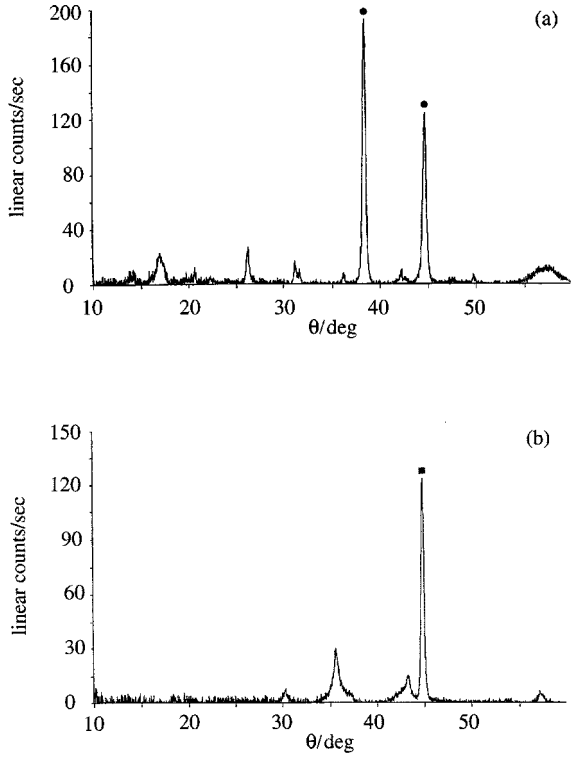

Figure 8 XRD of sample 5. (a) On silicon substrate; ●, aluminium sample holder. (b) On 35CD4 steel substrate; ■, substrate.

isothermal mode, the heating temperature was rapidly reached by using a heating rate of 20–30 K min^{-1}. The mass range of the QMS is from 1 to 200 amu.

Chemical vapor deposition

The deposition of thin films was carried out in a hot-wall CVD unit (Fig. 9). The reactor part consisted of a Pyrex or quartz tube (ϕ=25 mm) inserted into a Thermolyne tubular furnace (T_{max} 1473 K). The constant-temperature zone of the furnace was *ca* 8 cm long. The temperature of the furnace was regulated through an external PID system connected to a K-type thermocouple located between the furnace and the tube. Si(100) and 35CD4 steel substrates were used and located in the constant-temperature zone of the furnace. They were pretreated as follows: silicon substrates were cleaned in H_2SO_4/H_2O_2 (1:4), rinsed in distilled water and dried; steel substrates were polished mechanically using abrasive paper (grades 600 to 4000) and diamond paste, and sonicated in an ethanol bath. The unit was equipped with a liquid-nitrogen trap and a high-flow-rate primary pump (Edwards E2M12). A Pirani gauge indicated the total pressure of the system. The precursor driving system consisted of one U-type saturator immersed in a temperature-controlled oil bath. The saturator was loaded inside an argon-filled dry box in order to prevent, as much as possible, oxygen and water contamination. The line between the saturator and the reactor was heated to 10 K above the

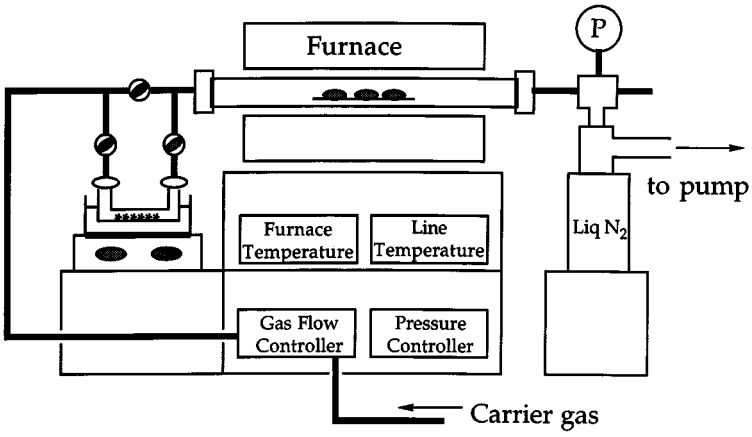

Figure 9 Schematic diagram of the CVD equipment.

vaporization temperature of the precursor in order to avoid recondensation. The precursor vapor was driven to the reactor by using nitrogen carrier gas. ASM mass flowmeters were used to control the gas flow rate. The saturator was equipped with a by-pass allowing connection to the unit and further purification without interaction with the precursor. The system was evacuated and refilled with the carrier gas three times before the carrier gas flow was opened to the precursor container and the furnace was heated. The precursor was heated at its vaporization temperature when the furnace had reached the desired temperature. At the end of the experiment (*ca* 2 h), the unit was cooled down to room temperature under gas flow.

Acknowledgements We are grateful to Dr P. Cassoux for his interest and support to this work. We thank S. Richelme and C. Claparols for MS analysis, G. Chatainier and E. Provincial for XPS data, D. Oquab for SEM/EDS studies, Ph. de Parseval for EPMA/WDS analyses, and J. Jaud and P. Baules for XRD data. This work was supported by the CNRS, the French Research and Education Ministry (PhD grant to B. C.), the DGA–DREG (G 8) of the French National Defense Ministry, and the Conseil Régional Midi-Pyrénées.

REFERENCES

1. C. H. Winter, J. W. Proscia, A. L. Rheingold and T. S. Lewkebandara. *J. Inorg. Chem.* **33**, 1227 (1994).
2. D. M. Hoffman, *Polyhedron* **13**, 1111 (1994).
3. G. S. Girolami, J. A. Jensen, D. M. Pollina, W. S. Williams, A. E. Kaloyeros and C. M. Alloca, *J. Am. Chem. Soc.* **109**, 1579 (1987).
4. L. V. Interrante, W. Lee, M. McConnell, N. Lewis and E. Hall. *J. Electrochem. Soc.* **136**, 472 (1989).
5. F. Laurent, J. S. Zhao, R. Choukroun and P. Cassoux. *J. Anal. Appl. Pyrol.* **24**, 39 (1992).
6. H. T. Chiu and S. H. Chuang. *J. Mater. Res.* **8**, 1353 (1993).
7. J. J. Ritter, J. F. Kelly, D. E. Newbury and D. B. Minor. *Proc. Int. Conf. on 'Chemistry of Electronic Ceramic Materials'*, Jackson, W. Y., USA, 17–22 August 1990, issued January 1991.
8. R. M. Laine, B. J. Aylett, J. Livage, D. Schleich and R. J. P. Corriu, in: *Transformation of Organometallic Compounds into Common and Exotic Materials: Design and Activation*, Laine, R. M. (ed), Martinus Nijhoff, NATO ASI Series, 1986, p. 241.
9. L. E. Toth, *Transition Metal Carbides and Nitrides, Refractory Materials*, Margrave, J. L. (ed.), Academic Press, New York, 1971.
10. R. Juza in: *Advances in Inorganic Chemistry and Radiochemistry*, vol. 9, Emeleus, H. J. and Sharpe, A. G. (eds), Academic Press, New York, 1996, pp. 81–131.
11. S. P. Murarka. *Silicides for VLSI Applications*, Academic Press, Orlando, (1993).
12. S. P. Murarka *J. Vac Sci. Technol.* **B4**, 1325 (1986).
13. J. J. Nickl, K. K. Schweitzer and P. Luxenberg, *J. Less-Common Metals* **26**, 335 (1972).
14. T. Goto and T. Harai, *Mater. Res. Bull.* **22**, 1195 (1987).
15. S. Sambasivan and W. T. Petuskey, *J. Mater. Res.* **7**, 1473 (1992).
16. S. Sambasivan and W. T. Petruskey, *J. Mater. Res.* **9**, 2362 (1994).
17. G. Llauro, A. Bendeddouche, M. Nadal and R. Hillel, *J. Phys. IV* **C5**, 801 (1995).
18. M. Touanen, F. Teyssandier, M. Ducarroir, M. Maline and R. Hillel, *J. Amer. Ceram. Soc.* **76**, 1473 (1993) and references cited therein.
19. R. Pampush, J. Lis, J. Piekarczyk and L. Stobierski, *J. Mater. Synth. Proc.* **1**, 93 (1993).
20. C. Racault, F. Langlais and R. Naslain. *J. Mater. Sci.* **29**, 3384 (1994).
21. C. R. Bennett and D. C. Bradley, *J. Chem. Soc., Chem. Commun.* **29** (1974).
22. S. J. Simpson and R. A. Andersen, *Inorg. Chem.* **20**, 3627 (1981).
23. C. D. Wagner, *Handbook of X-ray Photoelectron Spectroscopy*, Muilenberg, G. E. (ed.), Perkin-Elmer Corporation, 1979.
24. M. Woydt, A. Skopp and K. H. Habig, *Wear* **148**, 377 (1991).

